Annals of Pure and Applied Mathematics
Vol. 3, No. 2, 2013, 129-141
ISSN: 2279-087X (P), 2279-0888(online)
Published on 21August 2013
www.researchmathsci.org

Annals of
Pure and Applied Mathematics

MHD Free Convection and Mass Transfer Flow with Heat Generation through an Inclined Plate

Md. Saidul Islam [1], ***Md. Samsuzzoha*** [2], ***Shamim Ara*** [3] **and** ***Pinakee Dey*** [4]

[1]Department of Mathematics, Faculty of Science
Engineering & Technology, Hamdard University Bangladesh, Bangladesh
[2]Department of Mathematics, Faculty of Engineering & Industrial Science Swinburne University of Technology, Hawthonn, Victoria-3122, Australia
[3]Department of Mathematics, University of Rajshahi
Rajshahi-6205, Bangladesh
[4]Department of Mathematics, Mawlana Bhasani Science and Technolog University, Santosh, Tangail, Bangladesh.
E-mail: saeedmathku@yahoo.com

Received 4 August 2013; accepted 20 August 2013

Abstract. The numerical study is performed to examine the steady two-dimensional MHD free convection and mass transfer flow past through an inclined plate with heat generation. The governing partial differential equations are transformed to a system of dimensionless coupled partial differential equation. Finite difference method has been used to solve the above equations. The effects on the velocity, temperature, concentration distribution of various parameters entering into the problem separately are discussed with the help of graphs and tables.

Keywords: MHD, Convection, Heat Transfer, Magnetic parameter, Grashof number.

AMS Mathematics Subject Classification (2010): 80A20

1. Introduction

Investigation of Magneto hydrodynamic flow (MHD) for an electrically conducting fluid past a heated surface has attracted the interest of many researchers in view of its important applications in many engineering problems such as plasma studies, petroleum industries, MHD power generators, cooling of nuclear reactors, the boundary layer control in aerodynamics, and crystal growth. This study has been largely concerned with the flow and heat transfer characteristics in various physical situations. Alam and Sattar [1] investigated the heat transfer in thermal boundary layers of magneto-hydrodynamic flow over a flat plate. Elbashbeshy [2] studied heat and mass transfer along a vertical plate in the presence of a magnetic field. Chamkha and Khaled [3] investigated the problem of coupled heat and mass transfer by hydromagnetic free convection from an inclined plate in the presence of internal heat generation or absorption, and similarity solutions were presented.

The problem of free convection and mass transfer flow of an electrically conducting fluid past an inclined vertical surface under the influence of a magnetic field has attracted interest in view of its application to geophysics, astrophysics and many engineering problems, such as cooling of nuclear reactors, the boundary layer control in aerodynamics. Hossain et al. [4] studied the free convection flow from an isothermal plate inclined at a small angle to the horizontal. Anghel et al. [5] presented a numerical solution of free convection flow past an inclined surface. Reddy and Reddy [6] performed an analysis to study the natural convection flow over a permeable inclined surface with variable temperature, momentum and concentration. The study of the heat generation or absorption in moving fluids is important problems dealing with chemical reactions and those concerned with dissociating fluids. Vajravelu and Hadjinicolaou [7] studied the heat transfer boundary layer of a viscous fluid over a stretching sheet with internal heat generation. Hossain et al. [8] studied the problem of natural convection flow along a vertical wavy surface in the presence of heat generation/absorption.

Hence our aim is to study MHD free convection and mass transfer flow past through an inclined plate with heat generation.

2. Mathematical Formulation

By introducing Cartesian co-ordinate system, the $X-$axis is chosen along the plate in the direction of the flow and the $Y-$axis is normal to it. Initially it has been considered that the plate as well as the fluid is at the same temperature $T\left(T_\infty\right)$ and the concentration level $C\left(C_\infty\right)$ everywhere in the fluid is same. Also it is considered that the fluid and the plate is at rest after that the plate is to be moving with a constant velocity. U_0 in its own plane and instantaneously at time t > 0, the species concentration and the temperature of the plate are raised to $C_w\left(>C_\infty\right)$ and $T_w\left(>T_\infty\right)$ respectively, which are there after maintained constant, where C_w, T_w are species concentration and temperature at the wall of the plate and C_∞, T_∞ are the concentration and temperature of the species far away from the plate respectively. The physical configuration of the problem is shown in Fig 1. Within the framework of the above stated assumptions with reference to the generalized equations described before the equation relevant to the transient two dimensional problems are governed by the following system of coupled non-linear differential equations.

Continuity equation $\frac{\partial u}{\partial x}+\frac{\partial v}{\partial y}=0$ (1)

Momentum equation

$$\frac{\partial u}{\partial t}+u\frac{\partial u}{\partial x}+v\frac{\partial u}{\partial y}=v\frac{\partial^2 u}{\partial y^2}+g\beta\left(T-T_\infty\right)\cos\alpha+g\beta^*\left(C-C_\infty\right)\cos\alpha-\frac{\sigma\beta_0^2}{\rho}u \tag{2}$$

Energy equation $\frac{\partial T}{\partial t}+u\frac{\partial T}{\partial x}+v\frac{\partial T}{\partial y}=K_T\frac{\partial^2 T}{\partial y^2}+\frac{Q_T}{\rho C_p}$ (3)

Concentration equation $\frac{\partial C}{\partial t}+u\frac{\partial C}{\partial x}+v\frac{\partial C}{\partial y}=D\frac{\partial^2 C}{\partial y^2}$ (4)

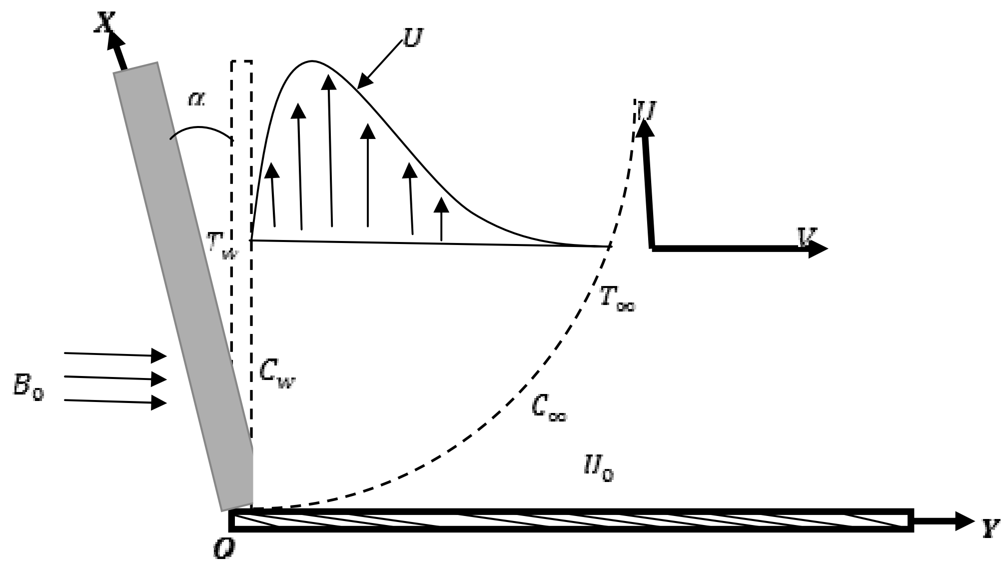

Fig. 1: The physical model and coordinate system

With the corresponding initial and boundary conditions are
at $t=0$ $u=0, v=0, C\to C_\infty$ everywhere5

$$
\begin{aligned}
& u=0,\ v=0,\ T\to T_\infty,\ C\to C_\infty \quad at\ x=0\\
t>0 \quad & u=U_0,\ v=0,\ T\to T_\infty,\ C\to C_\infty \quad at\ y=0 \qquad (6)\\
& u=0,\ v=0,\ T\to T_w,\ C\to C_w \quad as\ y\to\infty
\end{aligned}
$$

where x,y are Cartesian co-ordinate system. u,v are x,y component of flow velocity respectively. Here g is the local acceleration due to gravity ; υ is the kinematic viscosity; ρ is the density of the fluid ; K is the thermal conductivity ; C_p is the specific heat at the constant pressure; D is the coefficient of mass diffusivity.

Since the solutions of the governing equations (1)-(4) under the initial (5) and boundary (6) conditions will be based on a finite difference method it is required to make the said equations dimensionless.
For this purpose it has been now introduced the following dimensionless variables;

$$X=\frac{xU_0}{\upsilon},\ Y=\frac{yU_0}{\upsilon},\ U=\frac{u}{U_0},\ V=\frac{v}{U_0},\ \tau=\frac{tU_0^2}{\upsilon},\bar{T}=\frac{T-T_\infty}{T_w-T_\infty},Q_T=(T-T_\infty)Q^*$$

and $\bar{C}=\dfrac{C-C_\infty}{C_w-C_\infty}$

From the above dimensionless variable we have

$u=U_0U,\ T=T_\infty+\left(T_w-T_\infty\right)\bar{T}$ and $C=C_\infty+\left(C_w-C_\infty\right)\bar{C}$

Using these relations we have the following derivatives are

$$\frac{\partial u}{\partial t}=\frac{\partial u}{\partial \tau}\frac{\partial \tau}{\partial t}=U_0\frac{\partial U}{\partial \tau}\frac{U_0^2}{\upsilon}=\frac{U_0{}^3}{\upsilon}\frac{\partial U}{\partial \tau}$$

$$\frac{\partial u}{\partial x}=\frac{\partial u}{\partial X}\frac{\partial X}{\partial x}=U_0\frac{\partial U}{\partial X}.\frac{U_0}{\upsilon}=\frac{U_0{}^2}{\upsilon}\frac{\partial U}{\partial X}$$

$$\frac{\partial u}{\partial y}=\frac{\partial u}{\partial Y}\frac{\partial Y}{\partial y}=\frac{U_0{}^2}{\upsilon}\frac{\partial U}{\partial Y}$$

$$\frac{\partial^2 u}{\partial y^2}=\frac{\partial}{\partial y}\left(\frac{\partial u}{\partial y}\right)=\frac{\partial}{\partial y}\left(\frac{U_0^2}{\upsilon}.\frac{\partial U}{\partial Y}\right)=\frac{\partial}{\partial Y}\left(\frac{U_0^2}{\upsilon}.\frac{\partial U}{\partial Y}\right).\frac{\partial Y}{\partial y}=\frac{U_0^3}{\upsilon^2}\frac{\partial^2 U}{\partial Y^2}$$

$$\frac{\partial v}{\partial y}=\frac{\partial v}{\partial Y}\frac{\partial Y}{\partial y}=\frac{U_0^2}{\upsilon}\frac{\partial V}{\partial Y}$$

$$g\beta\left(T-T_\infty\right)\cos\alpha=g\beta\left\{T_\infty+(T_w-T_\infty)\bar{T}-T_\infty\right\}\cos\alpha=g\beta(T_w-T_\infty)\bar{T}\cos\alpha$$

$$g\beta^*\left(C-C_\infty\right)\cos\alpha=g\beta^*\left\{C_\infty+(C_w-C_\infty)\bar{C}-C_\infty\right\}\cos\alpha=g\beta^*(C_w-C_\infty)\bar{C}\cos\alpha$$

$$\frac{\sigma\beta_0^2}{\rho}u=\frac{\sigma\beta_0^2}{\rho}U_0U$$

$$\frac{\partial T}{\partial x}=\frac{U_0\left(T_w-T_\infty\right)}{\upsilon}\frac{\partial \bar{T}}{\partial X};\ \frac{\partial T}{\partial y}=\frac{U_0\left(T_w-T_\infty\right)}{\upsilon}\frac{\partial \bar{T}}{\partial Y};$$

$$\frac{\partial^2 T}{\partial y^2}=\frac{U_0{}^2}{\upsilon^2}\left(T_w-T_\infty\right)\frac{\partial^2\bar{T}}{\partial Y^2};\ \frac{\partial C}{\partial t}=\frac{U_0{}^2}{\upsilon}\left(C_w-C_\infty\right)\frac{\partial \bar{C}}{\partial \tau}$$

$$\frac{\partial C}{\partial x}=\frac{U_0}{\upsilon}\left(C_w-C_\infty\right)\frac{\partial \bar{C}}{\partial X};\ \frac{\partial C}{\partial y}=\frac{U_0}{\upsilon}\left(C_w-C_\infty\right)\frac{\partial \bar{C}}{\partial Y};\ \frac{\partial^2 C}{\partial y^2}=\frac{U_0{}^2}{\upsilon^2}\left(C_w-C_\infty\right)\frac{\partial^2\bar{C}}{\partial Y^2}$$

Now, we substitute the values of the above derivatives into the equations (1)-(3) and by simplifying, it has been obtained the following nonlinear coupled partial differential equations in terms of dimensionless variables

$$\frac{\partial U}{\partial X}+\frac{\partial V}{\partial Y}=0 \tag{7}$$

$$\frac{\partial U}{\partial \tau}+U\frac{\partial U}{\partial X}+V\frac{\partial U}{\partial Y}=\frac{\partial^2 U}{\partial Y^2}+G_r\bar{T}\cos\alpha+G_m\bar{C}\cos\alpha-MU \tag{8}$$

$$\frac{\partial \bar{T}}{\partial \tau}+U\frac{\partial \bar{T}}{\partial X}+V\frac{\partial \bar{T}}{\partial Y}=\frac{1}{\Pr}\frac{\partial^2 \bar{T}}{\partial Y^2}+\bar{T}.\bar{\alpha} \tag{9}$$

$$\frac{\partial \bar{C}}{\partial \tau}+U\frac{\partial \bar{C}}{\partial X}+V\frac{\partial \bar{C}}{\partial Y}=\frac{1}{S_c}\frac{\partial^2 \bar{C}}{\partial Y^2} \tag{10}$$

where,

Grashof number $=G_r=\upsilon g\beta\dfrac{\left(T_w-T_\infty\right)}{U_0^{\,3}}$

Modified Grashof number $=G_m=\upsilon g^*\beta\dfrac{\left(C_w-C_\infty\right)}{U_0^{\,3}}$

Magnetic parameter $=M=\dfrac{\sigma\beta_0^2\upsilon}{U_0^2}$

Prandlt number $=\Pr=\dfrac{\upsilon\rho C_p}{K}$

Schmidt number $=S_c=\dfrac{\upsilon}{D}$

Also the associated initial and boundary conditions become

$$\tau=0 \quad U=0,\ V=0,\ \bar{T}=0,\ \bar{C}=0 \quad \text{everywhere} \tag{11}$$

$$\begin{aligned} & U=0,\ V=0,\ \bar{T}=0,\ \bar{C}=0 \quad at\ X=0 \\ \tau>0 \quad & U=0,\ V=0,\ \bar{T}=1,\ \bar{C}=1 \quad at\ Y=0 \\ & U=0,\ V=0,\ \bar{T}=0,\ \bar{C}=0 \quad as\ Y\to\infty \end{aligned} \tag{12}$$

3. Numerical Calculations

In this section, it has been attempted to solve the governing second order nonlinear coupled dimensionless partial differential equations with the associated initial and boundary conditions.

From the concept of the above discussion, for simplicity the explicit finite difference method has been used to solve equations (1) - (4) subject to the conditions given by (5) and (6). To obtain the difference equations the region of the flow is divided into a grid of lines parallel to X and Y axes where Y-axes is taken along the plate and X - axes is inclined to the plate. Here we consider that the plate of height $X_{\max}(=100)$ i.e. X varies from 0 to 100 and regard $Y_{\max}(=25)$ as corresponding to $Y\to\infty$ i.e. Y varies 0 to 25. There are $m=100$ and $n=100$ grid spacing in the X and Y directions respectively as shown in the Fig. 2.

It is assumed that ΔX, ΔY are constant mesh sizes along X and Y directions respectively and taken as follows,

$\Delta X = 1 (0 \le x \le 100)$

$\Delta Y = 0.2 (0 \le y \le 25)$

With the smaller time step, $\Delta\tau = 0.001$

Now $U', V', \bar{T}', \bar{C}'$ are denoted the values of $U, V, \bar{T}$ and $\bar{C}'$ at the end of a step of time respectively.

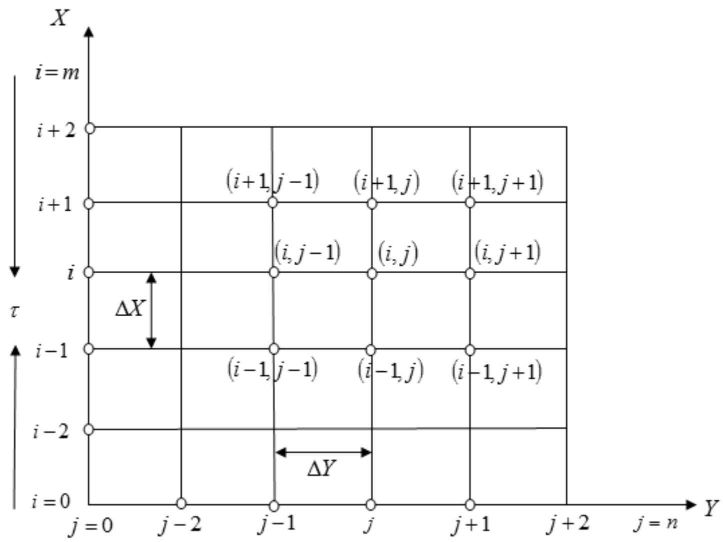

Fig. 2. The finite difference space grid

Using the explicit finite difference approximation we get,

$$\left(\frac{\partial U}{\partial \tau}\right)_{i,j} = \frac{U'_{i,j} - U_{i,j}}{\partial \tau}, \quad \left(\frac{\partial U}{\partial X}\right)_{i,j} = \frac{U_{i,j} - U_{i-1,j}}{\Delta X},$$

$$\left(\frac{\partial U}{\partial Y}\right)_{i,j} = \frac{U_{i,j+1} - U_{i,j}}{\Delta Y}, \quad \left(\frac{\partial V}{\partial Y}\right)_{i,j} = \frac{V_{i,j} - V_{i,j-1}}{\Delta Y},$$

$$\left(\frac{\partial \bar{T}}{\partial \tau}\right)_{i,j} = \frac{\bar{T}'_{i,j+1} - \bar{T}_{i,j}}{\Delta \tau}; \left(\frac{\partial \bar{T}}{\partial X}\right)_{i,j} = \frac{\bar{T}_{i,j} - \bar{T}_{i-1,j}}{\Delta X}; \left(\frac{\partial \bar{T}}{\partial Y}\right)_{i,j} = \frac{\bar{T}_{i,j+1} - \bar{T}_{i,j}}{\Delta \tau}$$

$$\left(\frac{\partial \bar{C}}{\partial \tau}\right)_{i,j} = \frac{\bar{C}'_{i,j} - \bar{C}_{i,j}}{\Delta \tau}; \left(\frac{\partial \bar{C}}{\partial X}\right)_{i,j} = \frac{\bar{C}_{i,j} - \bar{C}_{i-1,j}}{\Delta X}; \left(\frac{\partial \bar{C}}{\partial Y}\right)_{i,j} = \frac{\bar{C}_{i,j+1} - \bar{C}_{i,j}}{\Delta Y}$$

$$\left(\frac{\partial^2 U}{\partial Y^2}\right)_{i,j} = \frac{U_{i,j+1} - 2U_{i,j} + U_{i,j-1}}{(\Delta Y)^2}; \left(\frac{\partial^2 \bar{T}}{\partial Y^2}\right)_{i,j} = \frac{\bar{T}_{i,j+1} - 2\bar{T}_{i,j} + \bar{T}_{i,j-1}}{(\Delta Y)^2}$$

$$\left(\frac{\partial^2 \bar{C}}{\partial Y^2}\right)_{i,j} = \frac{\bar{C}_{i,j+1} - 2\bar{C}_{i,j} + \bar{C}_{i,j-1}}{(\Delta Y)^2}$$

Substituting the above relations into the corresponding differential equation we obtain an appropriate set of finite difference equations,

$$\frac{U_{i,j}-U_{i-1,j}}{\Delta X}+\frac{V_{i,j}-V_{i,j-1}}{\Delta Y}=0$$

$$\therefore V_{i,j}=V_{i,j-1}+\frac{U_{i,j}-U_{i-1,j}}{\Delta X}\Delta Y$$

$$\frac{U'_{i,j}-U_{i,j}}{\Delta\tau}+U_{i,j}\frac{U_{i,j}-U_{i-1,j}}{\Delta X}+V_{i,j}\frac{U_{i,j+1}-U_{i,j}}{\Delta Y}=\frac{U_{i,j+1}-2U_{i,j}+U_{i,j-1}}{\left(\Delta Y\right)^2}+$$

$$Gr\overline{T}_{i,j}\cos\alpha+Gm\overline{C}_{i,j}\cos\alpha-MU_{i,j}$$

13

$$U'_{i,j}=\left[\begin{array}{l}\frac{U_{i,j+1}-2U_{i,j}+U_{i,j-1}}{\left(\Delta Y\right)^2}+Gr\overline{T}_{i,j}\cos\alpha+Gm\overline{C}_{i,j}\cos\alpha-MU_{i,j}-U_{i,j}\frac{U_{i,j}-U_{i-1,j}}{\Delta X}-\\ V_{i,j}\frac{U_{i,j+1}-U_{i,j}}{\Delta Y}\end{array}\right]\Delta\tau$$

$$+U_{i,j} \tag{14}$$

$$\frac{\overline{T}'_{i,j}-\overline{T}_{i,j}}{\Delta\tau}+U_{i,j}\frac{\overline{T}_{i,j}-\overline{T}_{i-1,j}}{\Delta X}+V_{i,j}\frac{\overline{T}_{i,j+1}-\overline{T}_{i,j}}{\Delta Y}=\frac{1}{\Pr}\frac{\overline{T}_{i,j+1}-2\overline{T}_{i,j}+\overline{T}_{i,j-1}}{\left(\Delta Y\right)^2}+\overline{T}_{i,j}\overline{\alpha}$$

$$\overline{T}'_{i,j}=\left[\frac{1}{\Pr}\frac{\overline{T}_{i,j+1}-2\overline{T}_{i,j}+\overline{T}_{i,j-1}}{\left(\Delta Y\right)^2}+\overline{T}_{i,j}\overline{\alpha}-\overline{T}_{i,j}\frac{\overline{T}_{i,j}-\overline{T}_{i-1,j}}{\Delta X}-V_{i,j}\frac{\overline{T}_{i,j+1}-\overline{T}_{i,j}}{\Delta Y}\right]\Delta\tau+\overline{T}_{i,j} \tag{15}$$

$$\frac{\overline{C}'_{i,j}-\overline{C}_{i,j}}{\Delta\tau}+U_{i,j}\frac{\overline{C}_{i,j}-\overline{C}_{i-1,j}}{\Delta X}+V_{i,j}\frac{\overline{C}_{i,j+1}-\overline{C}_{i,j}}{\Delta Y}=\frac{1}{S_c}\frac{\overline{C}_{i,j+1}-2\overline{C}_{i,j}+\overline{C}_{i,j-1}}{\left(\Delta Y\right)^2}$$

$$\overline{C}'_{i,j}=\left[\frac{1}{\Pr}\frac{\overline{C}_{i,j+1}-2\overline{C}_{i,j}+\overline{C}_{i,j-1}}{\left(\Delta Y\right)^2}-U_{i,j}\frac{\overline{C}_{i,j}-\overline{C}_{i-1,j}}{\Delta X}-V_{i,j}\frac{\overline{C}_{i,j+1}-\overline{C}_{i,j}}{\Delta Y}\right]\Delta\tau+\overline{C}_{i,j} \tag{16}$$

The initial and boundary conditions with the finite difference scheme are

$$U^0_{i,j}=0,\ \ V^0_{i,j}=0,\ \ \overline{T}^0_{i,j}=0,\ \overline{C}^0_{i,j}=0 \tag{17}$$

$$\begin{aligned}&U^n_{0,j}=0,\ \ V^n_{0,j}=0,\ \ \overline{T}^n_{0,j}=0,\ \overline{C}^n_{0,j}=0\\ &U^n_{i,0}=1,\ \ V^n_{i,0}=0,\ \ \overline{T}^n_{i,0}=1,\ \ \overline{C}^n_{i,0}=1\\ &U^n_{i,L}=0,\ \ V^n_{i,L}=0,\ \ \overline{T}^n_{i,L}=0,\ \ \overline{C}^n_{i,L}=0\end{aligned} \tag{18}$$

where $L\to\infty$

Here the subscripts i and j designate the grid points with x and y coordinates respectively and the superscript n represents a value of time, $\tau=n\Delta\tau$

where $n = 0,1,2,3........$ From the initial condition (4), the values of U is known at $\tau = 0$. During any one time step, the coefficients $U_{i,j}$ and $V_{i,j}$ appearing in equations (13)-(16) are created as constants. Then at the end of any time-step $\Delta\tau$ the new velocity U', the new induced magnetic field V' at all interior nodal points may be obtained by successive applications of equations (14) - (16) respectively. This process is repeated in time and provided the time-step is sufficiently small, U, V should eventually converge to values which approximate the steady-state solution of equations (14)-(16). These converged solutions are shown graphically in figures (13) – (14).

4. Results and Discussion

The main goal of the computation is to obtain the steady state solutions for the non-dimensional velocity U, temperature $\overline{T}$ and concentration $\overline{C}$ for different values of Magnetic parameter (M), Prandtl number $(\Pr)$, Grashof number (Gr), Modified Grashof number (Gm), Schmidt number (Sc), Heat source parameter $(\overline{\alpha})$ and with the angle 0^0 and 60^0. For this purpose computations have been carried out up to dimensionless time τ = 80. Thus the solution for dimensionless time τ =80 is essentially steady state solutions. Along with the steady state solutions the solutions for the Velocity U versus Y, Temperature $\overline{T}$ versus Y, Concentration $\overline{C}$ versus Y are shown in below for different values of parameters. Here figures have been drawn for dimensional time τ = 10, 20 and 30.

Fig. 3 represents the velocity distributions for different values of Magnetic parameter $(M = 0.5, 1.0, 1.5)$, the values of $\Pr = 0.71$ (Prandtl number for saltwater at $20^0 C$) and another parameters Grashof number $(Gr = 3.00)$, Modified Grashof number $(Gm = 2.00)$, Schmidt number $(Sc = 0.60)$, Heat source parameter $(\overline{\alpha} = 0.2)$ are constant and with an inclined angle 0^0. In this figure, it is observed that velocity distribution increases with the increases of Magnetic parameter.

(a)

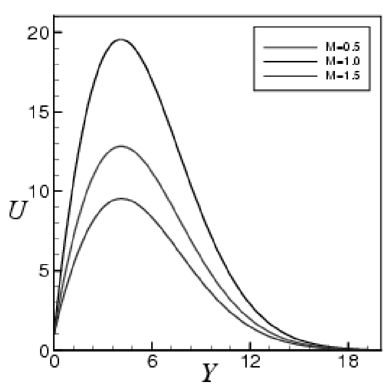

(b)

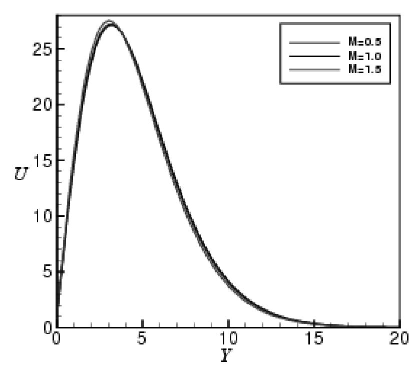

(c)

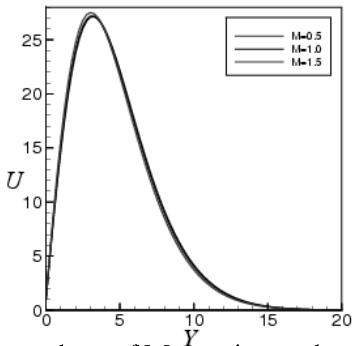

Fig. 3. Velocity profile different values of Magnetic number when *Gm* = 1, Gr= 2, $\bar{\alpha}$ = 0.5, *Sc* = 0.60, *Pr* = .71 and $cos\alpha$ = 1 at time (a) τ = 10, (b) τ = 20 and (c) τ = 30.

Fig.4 represents the velocity distributions for different values of Grashof number $(Gr = 2.0, 3.0, 4.0)$ and the values of $\Pr = 0.71$, $M = 0.5$, $Gm = 2.00$, $Sc = 0.60$, $\bar{\alpha} = 0.2$ are constant with an inclined angle 0^0. In this figure, it is observed that velocity distribution increases with the increases of Grashof number.

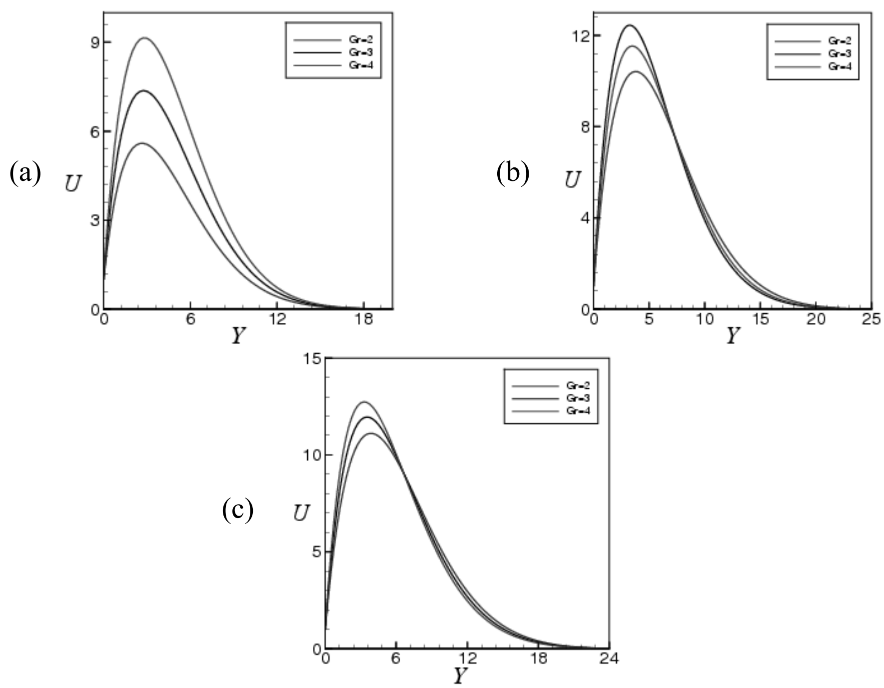

Fig. 4. Velocity profile different values of Grashof number when *Gm* = 2, *M*= 0.5, $\bar{\alpha}$ = 0.2, *Sc* = 0.60, *Pr* = .71 and $cos\alpha$ = 1 at time (a) τ = 10, (b) τ = 20 and (c) τ = 30

Fig. 5 represents the velocity distributions for different values of Prandtl number $(\Pr = 0.71, 1.0, 7.0)$ and the values of $M = 1.0$, $Gr = 3.00$, $Gm = 2.00$, $Sc = 0.60$, $\bar{\alpha} = 0.2$ are constant with an inclined angle 0^0. In this figure, it is observed that velocity distribution decreases with the increases of Prandtl number.

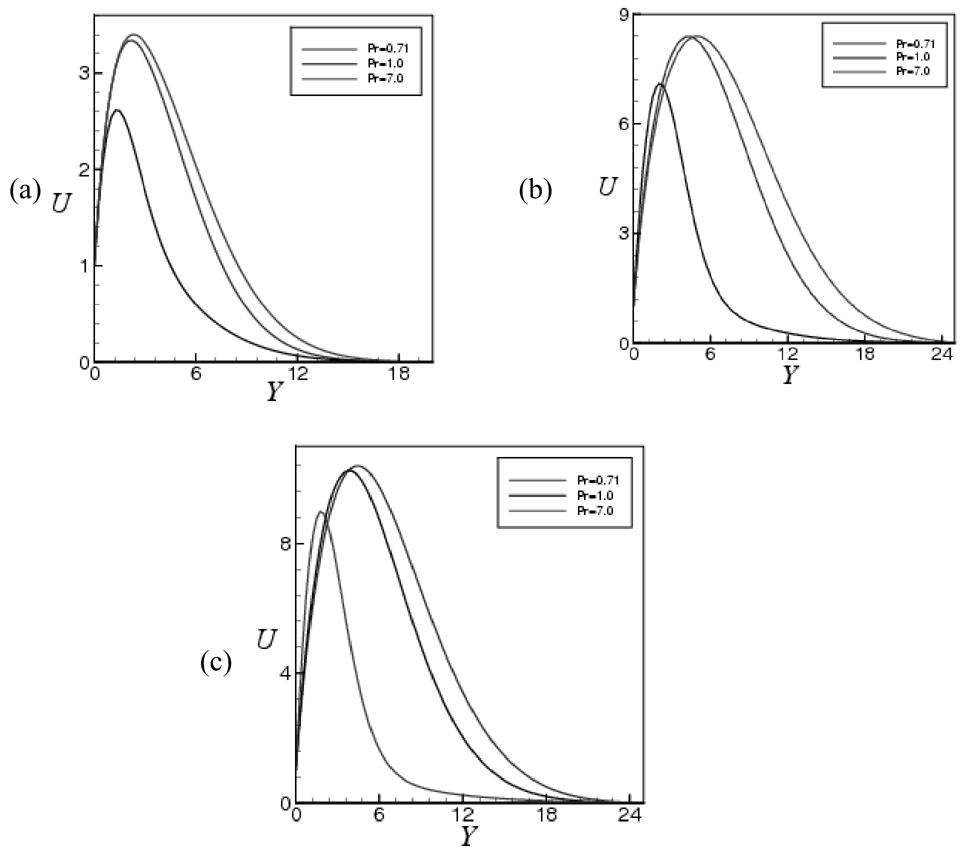

Fig. 5. Velocity profile different values of Pandlt number when *Gm* = 2, Gr= 2, *M*= 1, *Sc* = 0.60, $\bar{\alpha}$ = 0.2and $cos\alpha$ = 1 at time (a) τ = 10, (b) τ = 20 and (c) τ = 30

Fig.6 represents the velocity distributions for different values of Modify Grasshof number $Gm = 1.0, 2.0, 3.0$ and the values of when *Gr* = 2, *M*= 0.5, $\bar{\alpha}$ = 0.5, *Sc* = 0.60, *Pr* = .71 are constant with an inclined angle 0^0. In this figure, it is observed that velocity distribution increases at τ = 10 and remain constant at τ = 20 and τ = 30.

Fig. 7 represents the temperature distributions for different values of Heat source parameter $(\bar{\alpha} = 0.20, 0.50, 0.70)$ and the values of $\Pr = 0.71$, $M = 0.5$, $Gm = 1.00$, $Gr = 2.00$, $Sc = 0.60$ are constant with an inclined angle 0^0. In this figure, it is observed that temperature distribution increases with the increases of Heat source parameter.

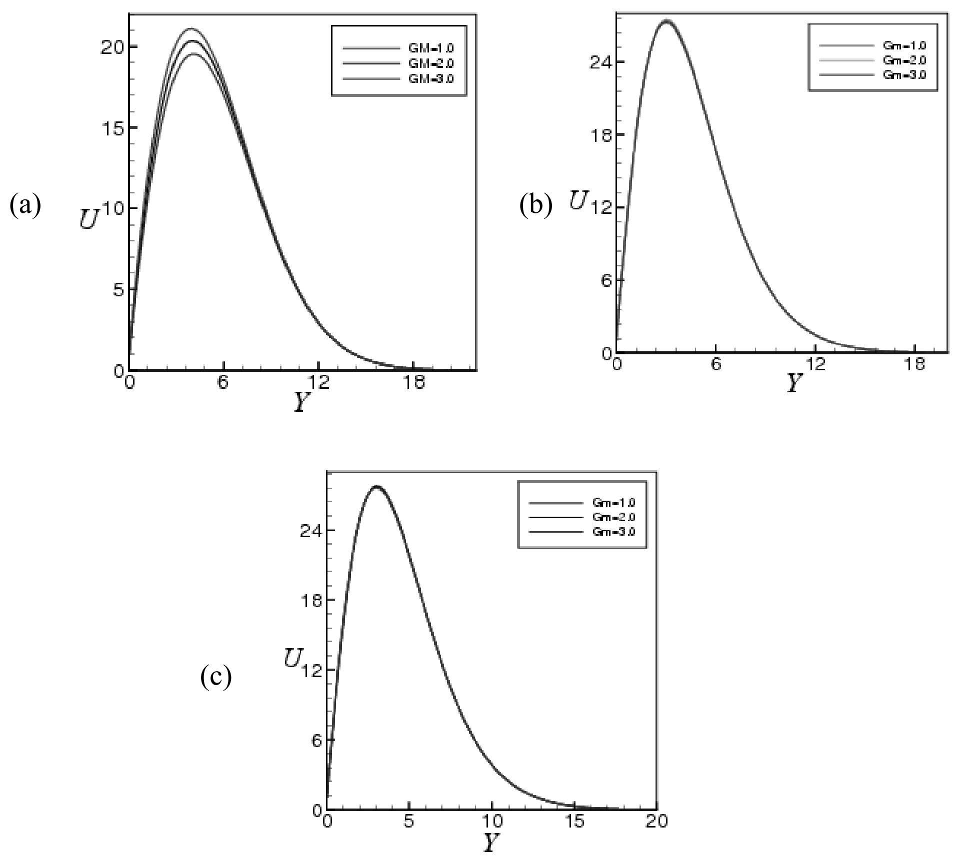

Fig. 6. Velocity profile different values of Modify Grasshof number when $Gr = 2$, $M= 0.5$, $\bar{\alpha} = 0.5$, $Sc = 0.60$, $Pr = .71$ and $cos\alpha = 1$ at time (a) $\tau = 10$, (b) $\tau = 20$ and (c) $\tau = 30$

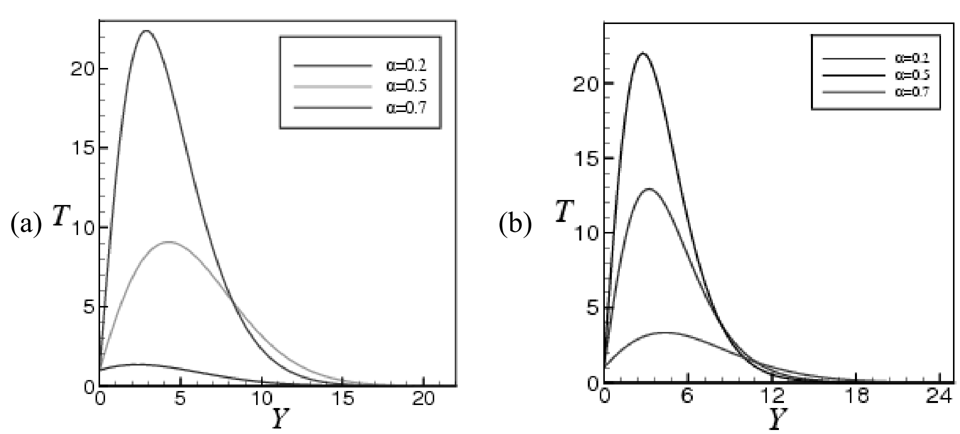

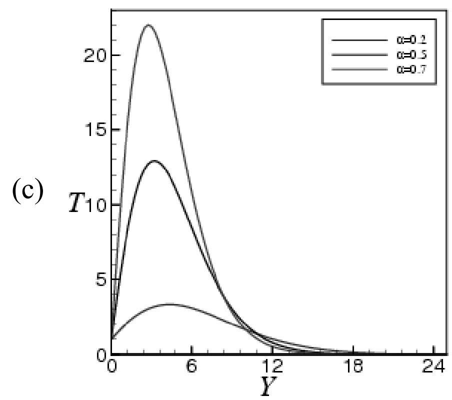

Fig. 7. Temperature profile for different values of Heat Source number when Gr = 2, Gm = 1,M= .5, Pr = .71 , Sc = 0.60 and $cos\alpha$ = 1 at time (a) τ = 10, (b) τ = 20 and (c) τ = 30

Fig.8 represents the temperature distributions for different values of Grashof number $(Gr = 2.0, 3.0, 4.0)$ and the values of $\Pr = 0.71$, $M = 0.5$, $Gm = 2.00$, $Sc = 0.60$, $\bar{\alpha} = 0.2$ are constant with an inclined angle 0^0. In this figure, it is observed that temperature distribution fluctuate with the increases of Grashof number.

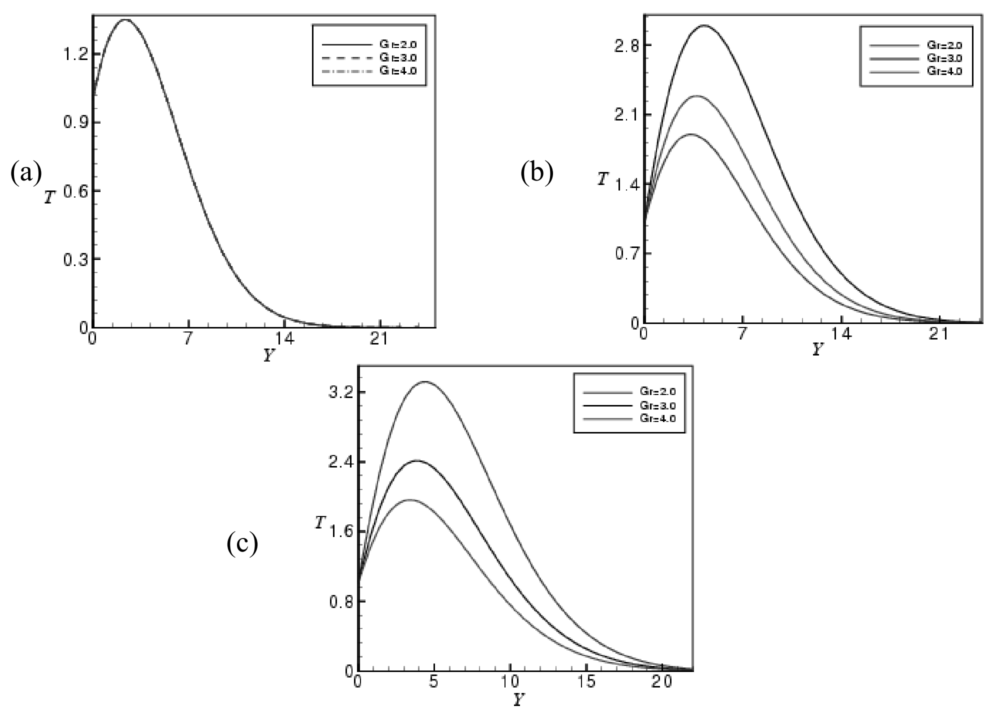

Fig. 8. Temperature profile for different values of Grassof number when $\bar{\alpha}$ = 0.2, Gm = 2,M= .5, Pr = .71 , Sc = 0.60 and $cos\alpha$ = 1 at time (a) τ = 10, (b) τ = 20 and (c) τ = 30

Fig. 9 represents the concentration distributions for different values of Magnetic parameter ($M = 0.5, 1.0, 1.5$) and the values of $\Pr = 0.71$, $Gr = 3.00$, $Gm = 2.00$, $Sc = 0.60$, $\overline{\alpha} = 0.2$ are constant with an inclined angle 0^0. In this figure, it is observed that there are no effects with the increase of Magnetic parameter.

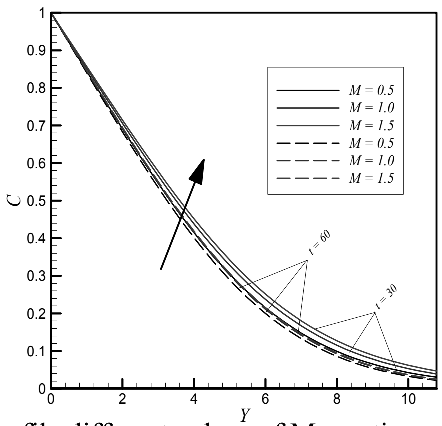

Fig. 9. Concentration profile different values of Magnetic number when Gm = 2, Gr= 3, $\overline{\alpha}$ = 0.2, Sc = 0.60, Pr = 0.71 and cosα = 1 at time τ = 30 and τ = 60.

5. Conclusion

In this report, it has been the studied equation of continuity and derived the Navier-Stoke equation of motion for viscous compressible and incompressible fluid flow. The boundary layer equation in two-dimensional flow, energy equation, mass transfer equations are obtained by boundary layer approximation. The velocity distribution increases with the increases of magnetic parameter while the temperature and concentration distribution increase with increase of Magnetic parameter. The velocity distribution increases with increases of Grashof number while temperature and concentration distribution decrease with increase of Grashof number. The velocity and temperature distribution increase with increase of Heat source parameter.

REFERENCES

1. M. M. Alam and M. A. Sattar, *J. of Energy, Heat and Mass Transfer*, 21 (1999), 9.
2. Elbashbeshy, *Int. J. Heat and Mass Transfer*, 19 (1997), 165.
3. Chamkha and Khaled, Simultaneous heat and mass transfer in free convection, *Industrial Engineering Chemical,* 49 (2001), 961-968.
4. Hossain et al (1996). MHD free convection flow from an isothermal plate, *J. Theo. and Appl. Mech.* 1, 94-207.
5. Angel et al., Combined heat and mass transfer in natural convection on inclined surfaces, *Numerical Heat Transfer,* 2 (2001), 233–250.
6. M.G. Reddy and N.B. Reddy, *Journal of Applied Fluid Mechanics*, 4 (2011) ,7- 11.
7. Vajravelu, K. and A. Hadjinicolaou, Heat transfer in a viscous fluid, *Int. Comn. Heat Mass Transfer,* 20 (1993), 417-430.
8. Hossain et al., Natural convection flow of heat generation, *Int. Them. Sci.,* 43, (2004) 157-163.